JACS
JOURNAL OF THE AMERICAN CHEMICAL SOCIETY
pubs.acs.org/JACS

Article

Valence Bond Theory Allows a Generalized Description of Hydrogen Bonding

Sason Shaik,* David Danovich, and Richard N. Zare*

Cite This: J. Am. Chem. Soc. 2023, 145, 20132−20140

Read Online

ACCESS | Metrics & More | Article Recommendations | Supporting Information

ABSTRACT: This paper describes the nature of the hydrogen bond (HB), B:---H−A, using valence bond theory (VBT). Our analysis shows that the most important HB interactions are polarization and charge transfer, and their corresponding sum displays a pattern that is identical for a variety of energy decomposition analysis (EDA) methods. Furthermore, the sum terms obtained with the different EDA methods correlate linearly with the corresponding VB quantities. The VBT analysis demonstrates that the total covalent-ionic resonance energy (RE_{CS}) of the HB portion (B---H in B:---H−A) correlates linearly with the dissociation energy of the HB, ΔE_{diss}. In principle, therefore, RE_{CS}(HB) can be determined by experiment. The VBT wavefunction reveals that the contributions of ionic structures to the HB increase the positive charge on the hydrogen of the corresponding external/free O−H bonds in, for example, the water dimer compared with a free water molecule. This increases the electric field of the external O−H bonds of water clusters and contributes to bringing about catalysis of reactions by water droplets and in water-hydrophobic interfaces.

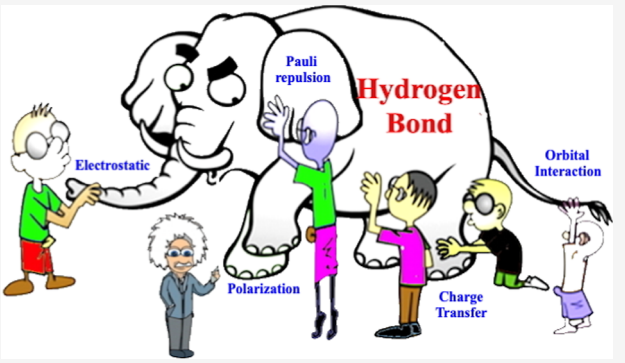

INTRODUCTION

There is a parable of Indian origins about a group of blind men encountering an elephant for the first time.[1,2] Each person touches a different part of the animal and makes wildly wrong assumptions about what the whole elephant looks like. In many ways, this parable applies to the enigmatic description of the origins of the hydrogen bond (HB).[1] The HB is often considered to be dominated by electrostatic (ES) interactions, polarization (POL), or covalent interactions in which electrons are shared to make a weak chemical bond. In this study, we show that ionic structures and covalent-ionic resonance energies[3] make more important contributions than have been previously known. Specifically, we find that using valence bond theory (VBT)[3,4] considers the HB to be sustained by covalent-ionic resonance energy,[3] arising from the combined charge transfer and POL effects. This resonance energy is, in principle, available from experiments (see Figure 5). Thus, we are able to present a unified picture of what a HB is. This description covers both strong and weak HBs. The ionic character helps to explain phenomena that have seemed unrelated and somewhat enigmatic; for example, how water in contact with some hydrophobic medium, such as air, oil, or a metal oxide surface, can become "electrified" and drive redox reactions that do not occur in bulk water.[5]

Brief Review of the Importance and Origins of HBs. The existence of HBs was postulated early on,[6] based on the Lewis theory of the chemical bond.[6b] Because hydrogen can make only a single bond, Pauling[7a] initially ruled out any bonding and defined the HB as an ES bond. However, in the 1960 edition of his book,[7b] he presented HB's using resonance theory. For example, Pauling described the water dimer in Scheme 1, using resonance structures **A**−**C**, but estimated **C**

Scheme 1. HB between Two Water Molecules; λ and δ Are the Small Contributions of B and C

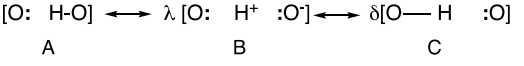

(based on the HB distance and the weight of the ionic contribution to the O−H bond) to be marginally 5%.[7b] However, we show in this study that both structure **C** and the corresponding resonance energy of the HB portion are very significant.

Recognition of the importance of HBs in chemistry has quickly grown. The HB constitutes a key architectural element of matter (e.g., in ice, proteins, and nucleic acids) and it is responsible for the stability of aggregates of small molecules (e.g., heats of vaporization of water and hydrofluoric acid (HF)

Received: July 30, 2023
Published: September 4, 2023

https://doi.org/10.1021/jacs.3c08196
J. Am. Chem. Soc. 2023, 145, 20132−20140

versus their heavier isoelectronic analogues).[8,9] HBs also endow matter with special mechanical properties in solution, solids, and polymers.[10]

Indeed, the identification of the interactions that dominate the strength of the HB and of bonds in general has remained a contentious issue and a source of many discussions.[9f,g,11,12] Generally speaking, there are two theoretical schools of thought in calculating the strength of HBs.

One school of thought has emerged from the energy decomposition analysis (EDA) schemes of Kitaura−Morokuma,[13] Ziegler−Rauk,[14] and Baerends−Bickelhaupt.[15] EDA methods analyze the HB interaction in terms of ES, POL, Pauli repulsion (EX), charge transfer (CT), and orbital interactions.[15] By Pauli's repulsion, it is meant that no two electrons may simultaneously occupy the same quantum state so that when brought together they experience a repulsive interaction.

Commonly used EDA methods emphasize the ES origin of HBs. Similarly, the block-localized wavefunction (BLW) method of Mo et al.,[16] which is akin to VBT using fragment orbitals,[4] was used to study relatively weak HBs,[17a] and the results were compared with those emerging from classical VBT calculations.[17b,c] The combined BLW and VBT studies showed that the interaction energies of these weak HBs are dominated by the ES (dipole−dipole) interactions with minor contributions from CT.

The second school of thought is based on the natural bond orbital (NBO) theory,[9e,18,19] which uses second-order perturbation theory to evaluate the interaction energy of the HBs (B: H−A) in terms of the interactions of the donor-occupied orbital n_B and the acceptor vacant bond orbital, σ_{HA}^*. The interaction energy is proportional to the square of the Fock (**F**) matrix element and inversely proportional to the NBO orbital energy gap

$$\Delta E_{int} = \frac{-2|<n_B|\boldsymbol{F}|\sigma_{HA}^*>|^2}{E(\sigma_{HA}^*) - E(n_B)} \quad (1)$$

As such, NBO theory predicts that the interaction energy (ΔE_{int}) is dominated by the CT terms from the donor to the acceptor. ΔE_{int} in eq 1 is clearly a resonance term owing to the interactions of the orbital on B: (n_B) with the antibonding orbital of H−A (σ_{HA}^*). The related natural EDA (NEDA) method[20] supports the NBO conclusion that CT is important, but it gives rise to other energy terms, and specifically to a significant ES term.[9g]

The same dichotomy exists for the halogen bond (XB) interaction, where a halogen X atom bridges to two moieties B and A (B: X−A). A recent analysis of the XB interaction in terms of BLW and VBT[21] concluded that in most of the studied XB species, the CT is highly significant, if not the dominant stabilizing term. However, weaker XBs, which were studied by Grabowski,[9g,11] showed that the POL term is more important than CT. Another concept is the σ-hole, which predicts the linearity of the X-bonded clusters [B---X−Y], caused by the positive charge of the halogen (X) at the tip of its bond axis X−Y.[9g,11,22] As such, the σ-hole−XY interaction can be considered an ES.

The analysis of total interaction energy into many model terms is bound to create some ambiguities and disagreements (e.g., the effective one-electron operator, the Fock operator in eq 1, includes mono-electronic terms and effective bi-electronic ones). Recently, Pendas et al.[12a] developed the interacting quantum atoms (IQA) method, which is free of the problematic issues of other EDA methods (e.g., the violation of the Pauli exclusion rule for intermediate wavefunctions used to estimate the EDA energy term). The emerging QM atoms and fragments from the IQA method are well-defined by the quantum theory of atoms in molecules (QTAIM).[23] Using the interaction in HF---HF as an example,[12a] Pendas et al. demonstrated that different combinations of the various energy terms can lead to different conclusions about the nature of the HB. Their energy partitions showed that this moderately strong HB may be considered to be dominated by resonance CT or by ES interactions, depending on the groupings of the energy terms. Indeed, Foroutan-Nejad et al.[12b−d] demonstrated this path dependency for other bonding interactions. The path dependency obviously poses interpretational ambiguities for EDA.

VB Outlook of HBs. The present work avoids ambiguities by focusing on the nature of the HB, with the aim of unifying the various approaches and providing a lucid description of the HB in terms of VBT. We selected a series of HBs, which are collected in Scheme 2 and range from weak to strong, such as $(FHF)^-$ and $(HOHOH)^-$, which are symmetric (or nearly so) HBs[9g,24] and are most likely to be electronically delocalized species.

Scheme 2. HB Dimers Selected for This Study[a]

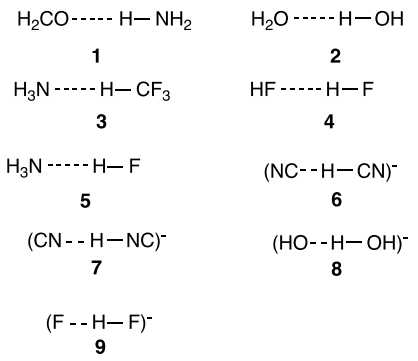

[a]HBs **6**−**9** have nearly symmetric geometries.

The nature of the HB will be determined here by means of classical VBT, which includes covalent and ionic structures. To compare our VB results/conclusions with those from other EDA methods, we studied the various HBs by means of the absolutely localized molecular orbitals (ALMO)-EDA,[25] NEDA,[20] and BLW[16] methods.

A merit of VBT[4] is that its treatment of the nature of the HB does not use intermediate wavefunctions that violate the Pauli exclusion principle, and at the same time, it uses chemically lucid VB structures. The main character of the HB is the sum of POL and covalent-ionic resonance energy owing to CT and POL. This sum creates a uniform interaction-energy pattern for the nine HBs shown in Scheme 2, and this uniformity is common to a variety of EDA methods (see Figure 3).

The VBT interaction involves chemical structures that flesh out POL and ionic features and provide clearly defined resonance energies that are related to experimental quantities that will be discussed below.[5,26] Finally, the VB treatment describes the HB as an electron-pair bond,[3] and we demonstrate that the VB-determined electron-pair bonding of the HB correlates linearly with the dissociation energy of the HB, and as such, the bonding is linked to this observable

https://doi.org/10.1021/jacs.3c08196
J. Am. Chem. Soc. 2023, 145, 20132−20140

quantity, which in principle can be determined by experimental means. It is this connection that has not been systematically emphasized in past treatments of this central topic in chemistry and biology. Among better known properties, such as the geometry and strength of the HB, we address the role of covalent-ionic mixing and POL in H-bonded water molecules in water-hydrophobic matter interfaces and water droplet surfaces.[5,26]

METHODS

Geometry Optimization. The HBs were optimized at the MP2[27] and CCSD(T)[28] levels of theory with the cc-pVTZ basis set.[29a] Details are collected in the Supporting Information.

VB Calculations. Classical VB calculations were performed with the XMVB program[30] using the breathing-orbital VB (L-BOVB) method[31] and the 6-311G(p,d) basis set.[29b] We note that the L-BOVB/6-311G(p,d) results for the dissociation energies of the HBs are slightly overestimated vis-à-vis the CCSD(T)/cc-pVTZ quantities. The CCSD(T)/6-311G(p,d) calculated dissociation energies also slightly overestimate the values calculated with CCSD(T)/cc-pVTZ (see Table S10 in the Supporting Information), but the trends in the HB strengths are identical. The following two VB spaces were tested:

(a) VB(6): here the HBs, B:-----H−A, were uniformly treated with an active VB space that includes the σ-lone pair of the donor (B: or B:$^-$) and the σ-bond-pair of the H−A bond. This leads to six VB structures, which are displayed in Scheme 3a for cases where B: is a neutral molecule (e.g., water and HF), and Scheme 3b where B:$^-$ is an anion (e.g., F:$^-$ and HO:$^-$).

Scheme 3. Six VB Structures Used for the VB(6) Level, Which Involves Four Valence Electrons, for B: or B:$^-$ Interacting with H−A; (a) 1−6 for a Neutral B:; (b) 1_a−6_a for an Anionic B:$^-$; the Arched Lines in Structures 4 (4_a) and 6 (6_a) Signify Covalent Bond-Coupling of the Respective Two Odd Electrons on B, H, and A; and Drawings of the σ-fragment Orbitals of the HB Are Presented on the Right Side

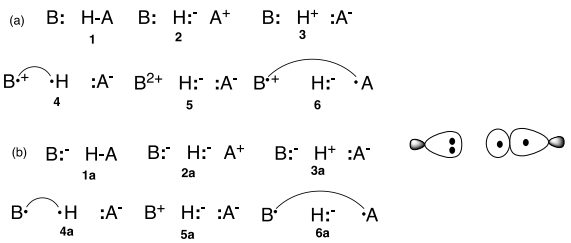

(b) VB(50): the minimal VB(6) active space was tested for HF:-----H−F against VB(50), which includes the two electrons of the left-side H−F bond in addition to the 4-electrons used for VB(6) [see Supporting Information for nonzero weighted structures in VB(50)]. The test showed that VB(6) is reasonably accurate.

Note that structures **1**−**3** ($\mathbf{1_a}$−$\mathbf{3_a}$) in Scheme 3 constitute the VB structures that describe the Lewis bond in the H−A molecule [Φ_L(H−A)]. The structures **3**−**5** ($\mathbf{3_a}$−$\mathbf{5_a}$) in Scheme 3 constitute the electron-pair wavefunction of the B----H bond [Φ_L(B----H)]. The corresponding wavefunction Φ_L(B----H) of the HB will account for the total resonance energy of the incipient HB (see Supporting Information). As described above, this quantity varies in correlation with the dissociation energy (ΔE_{diss}) of the HB and will establish a link between the VB-derived HB description and the experimental quantity that gauges the strength of the HB. Note that structure **6** ($\mathbf{6_a}$) will contribute additional resonance energy, but it was not included in the wavefunction of Φ_L(B----H) because its contributed resonance energy should be minor owing to the long distance of the paired electrons over B and A.

RESULTS AND DISCUSSION

Geometries and Charge Distributions of HBs (1−9). The charges of the optimized HB structures (at the BOVB and CCSD levels) are collected in Figure 1 (the bond lengths and

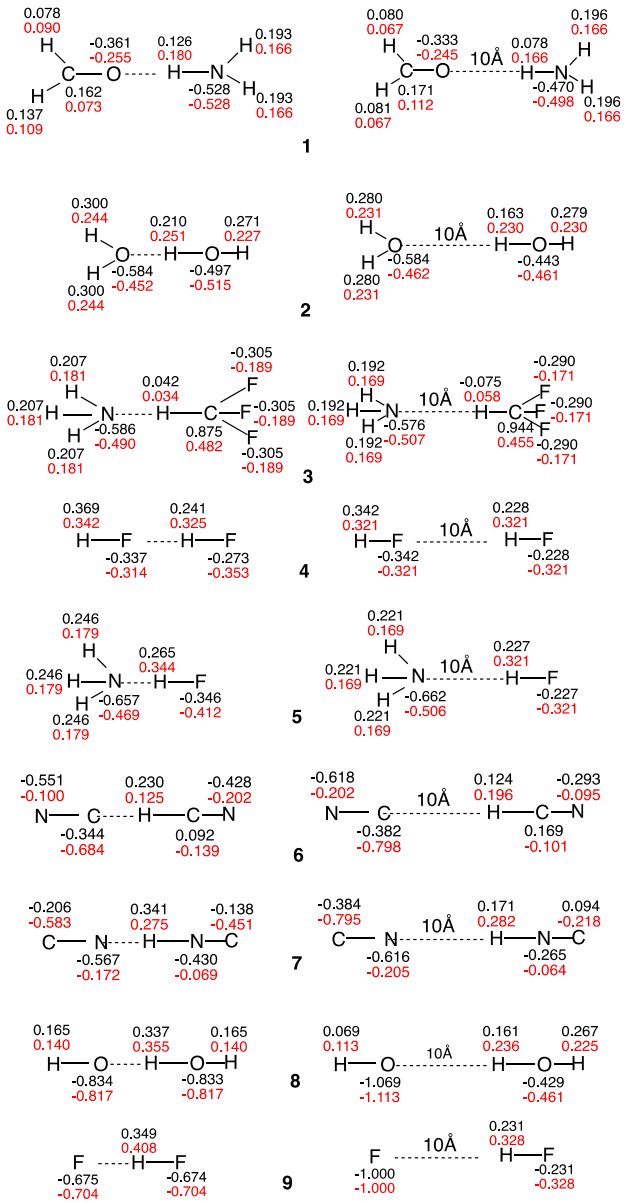

Figure 1. Mulliken charges (BOVB in black and CCSD in red) in the equilibrium geometries of HBs and their dissociated fragments (the distance is 10 Å). Numbers in the bold font near the species correspond to the HB numbers in Scheme 2.

Cartesian coordinates of the optimized HB structures are presented in the Supporting Information). The charges at both levels are often quite similar. The interesting features are that the geometries vary from asymmetric structures, such as the weak HB in the HF:-----H−F species, all the way to symmetric ones, such as the anionic species (F---H---F)$^-$. In some cases, for example, in the H_2O dimer (**2**, Figure 1), the hydrogen atoms outside of the HB carry higher positive charges than the Hs in the free molecule (which are represented by the 10 Å

https://doi.org/10.1021/jacs.3c08196
J. Am. Chem. Soc. 2023, 145, 20132−20140

distances in Figure 1). The symmetric and rather tight species arise from the dominance of the triple ionic VB structures, for example, F^- H^+ F^- in $(F{-}{-}{-}H{-}{-}{-}F)^-$.[32] On the other hand, the increased positive charges of the outer Hs, as in the water dimer $H_2O{-}{-}{-}H{-}OH$, originate in VB structure **4**, which is the covalent structure for the $H_2O{-}{-}{-}H$ bonds, and it has a positive charge on H_2O (B in **4**; Scheme 3a). This positive charge is related to observed redox reactions on the surfaces of water droplets.[5,26e,f]

Energy Diagrams of HBs. The energy partition for the HBs in Scheme 2 follows the same philosophy used before for halogen bonds.[21] As such, we use an economical energy decomposition, which involves the following four steps that are labeled in the energy diagram in Figure 2 and the energy terms in Table 1.

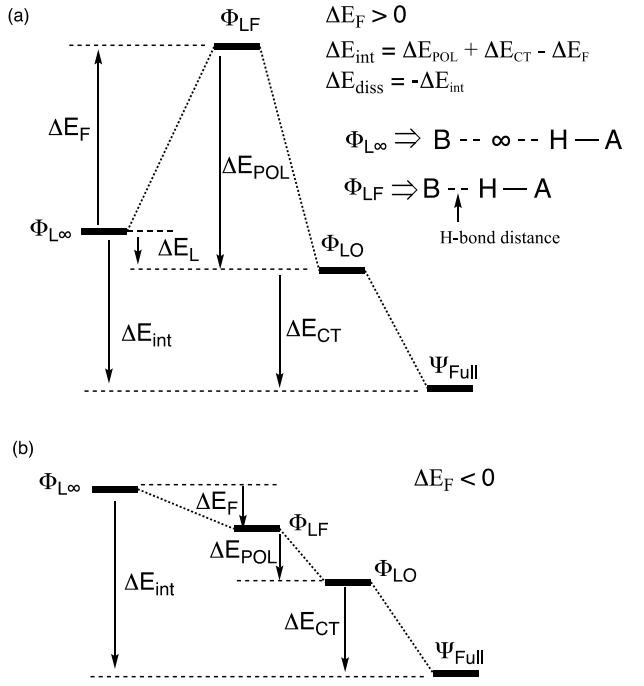

Figure 2. Energy diagrams of HBs with the corresponding energy partition quantities (ΔE_F, ΔE_{POL}, and ΔE_{CT}): (a) the diagram for seven HBs (**1**, **4**, and **5**–**9**). (b) Diagram for $H_2O{-}{-}{-}HO{-}H$ (**2**) and $H_3N{-}{-}{-}HCF_3$ (**3**). In both (a) and (b), Φ_{LO} is an optimized Lewis state at the HB distance, whereas Ψ_{full} corresponds to the full BOVB wavefunction, allowing mixing of VB structures **4**–**6**/$\mathbf{4_a}$–$\mathbf{6_a}$ into Φ_L.

Table 1. BOVB/6-311G(p,d) Energy Components (in kcal/mol), ΔE_F, ΔE_L, ΔE_{POL}, and ΔE_{CT}, of the HB Energies in 1–**9**

HB	ΔE_{POL}	ΔE_{CT}	ΔE_{diss}[a]	ΔE_F	ΔE_L	$\Delta E_{CT} + \Delta E_{POL}$
1	−23.16	−1.87	3.14	21.90	−1.27	−25.03
2	−2.23	−1.66	6.00	−2.10	−4.33	−3.89
3	−3.68	−2.61	6.50	−0.21	−3.89	−6.29
4	−9.87	−3.84	7.38	6.32	−3.55	−13.71
5	−15.00	−7.83	15.43	7.40	−7.61	−22.83
6	−19.90	−8.83	21.47	7.26	−12.64	−28.73
7	−61.86	−26.06	29.23	58.68	−3.17	−87.92
8	−72.62	−28.73	37.95	63.40	−9.23	−101.35
9	−60.46	−44.71	58.86	46.30	−14.15	−105.17

[a]ΔE_{diss} was calculated using eq 6. Identical results are obtained from Figure 2.

Initially, we use VB structures **1**–**3**/$\mathbf{1_a}$–$\mathbf{3_a}$ (Scheme 3) and calculate the Lewis state, $\Phi_{L\infty}$, in which the H–A bond is infinitely separated from B:. In practice, however, when the distance is 10 Å, the wavefunction does not involve contributions from structures **4**–**6**/$\mathbf{4_a}$–$\mathbf{6_a}$ and is considered effective infinite separation (see Supporting Information, Table S17).

We subsequently bring B: (B:$^-$) to the HB distance while freezing the orbitals of the VB wavefunction, which correspond to the base (B:/B:$^-$) and the Lewis bond (H–A), while allowing geometry optimization using the respective VB structures (**1**–**3** or $\mathbf{1_a}$–$\mathbf{3_a}$) of the Lewis bond H-A. This generates Φ_{LF}, which is the Lewis state at the equilibrium distance of the HB, but with frozen orbitals and Lewis VB structures as in the optimized Lewis state at infinity (10 Å).

The energy change (Figure 2) that accompanies the transformation of the wavefunction from $\Phi_{L\infty}$ to Φ_{LF} is ΔE_F. This quantity sums the Pauli repulsion between the H-A molecule and the base (B:), the deformation energies of the molecule and the base, and the ES stabilization that arises by bringing these moieties to the HB distance. For most of the HBs we investigated, $\Delta E_F > 0$ (Figure 2a), but in two cases ($H_2O{-}{-}{-}HOH$, **2**; $H_3N{-}{-}{-}HCF_3$, **3**) ΔE_F is negative (Figure 2b). In the latter cases, ES interactions are apparently large enough to overcome the repulsive factors and lead to a negative ΔE_F quantity.

Subsequently, by optimizing the Lewis structures of Φ_{LF} at the HB distance, we obtain the optimized Lewis state Φ_{LO}, where O signifies that the VB structures and orbitals of the Lewis states are optimized for the final HB geometry. This procedure changes the contributions of the individual VB structures within the Lewis wavefunction and brings about the POL of the respective wavefunction, thus resulting in the corresponding energy-lowering ΔE_{POL} (Figure 2).

Thereafter, by allowing the mixing of structures **4**–**6**/$\mathbf{4_a}$–$\mathbf{6_a}$ into the Lewis state (with further geometry optimization), we obtain the full wavefunction (Ψ_{full}), wherein the HB is fully represented. The energy is further lowered by the respective CT mixing energy, ΔE_{CT} (Figure 2).

The various energy terms in Figure 2 are as follows

$$\Delta E_{POL} = E(\Phi_{LO}) - E(\Phi_F) \quad (2)$$

$$\Delta E_{CT} = E(\Psi_{full}) - E(\Phi_{LO}) \quad (3)$$

$$\Delta E_F = E(\Phi_{LF}) - E(\Phi_{L\infty}) \quad (4)$$

$$\Delta E_L = E(\Phi_{LO}) - E(\Phi_{L\infty}) \quad (5)$$

$$\Delta E_{diss} = -\Delta E_{int} = -[E(\Psi_{full}) - E(\Phi_{L\infty})] \quad (6)$$

Table 1 shows the energy terms for the HBs in Scheme 2. Inspection of the data reveals that, with the exception of $H_2O{-}{-}{-}HOH$ and $H_2C{=}O{-}{-}{-}HNH_2$ (**2** and **3**), the ΔE_F quantity is positive and it destabilizes the Lewis state, Φ_{LF}. Relative to Φ_{LF}, the most important stabilizing factor is the ΔE_{POL} term, while ΔE_{CT} is a secondary stabilizing effect. Table 1 also shows the sum term $\Delta E_{CT} + \Delta E_{POL}$.

Sum Term ($\Delta E_{POL} + \Delta E_{CT}$) Unifies the Trends in the Nine HBs Examined. It is important to realize that different methods (e.g., BOVB, ALMO-EDA, NEDA, and BLW) do not fully agree with one another about whether the dominant stabilizing term is ΔE_{POL} or ΔE_{CT} in a particular HB. By contrast, as shown in Figure 3, all the methods reveal that the

https://doi.org/10.1021/jacs.3c08196
J. Am. Chem. Soc. 2023, 145, 20132−20140

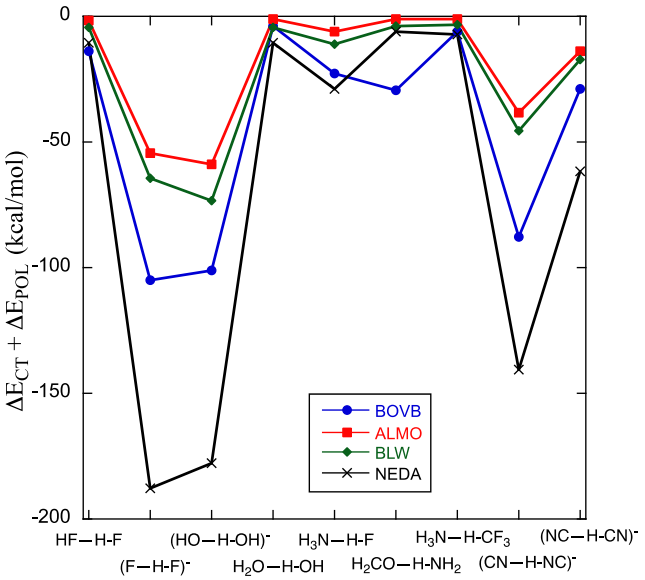

Figure 3. Pattern plot of the sum terms, $\Delta E_{CT} + \Delta E_{POL}$, for the family of HBs studied here (specified at the bottom of the plot).

sum of the terms, $\Delta E_{CT} + \Delta E_{POL}$, exhibits a very similar pattern for the variation of the stabilizing factor across the series of HBs. Thus, ΔE_{POL} and ΔE_{CT} are entangled, and their relative magnitudes may be path-dependent, but their sum exhibits consistency of patterns for all the HBs studied here. This behavior represents a major advance in our understanding of the nature of the HB.

Furthermore, the sum terms, $\Delta E_{CT} + \Delta E_{POL}$, calculated by various methodologies, correlate linearly with one another (see Figure S2 in the Supporting Information). Figure 4 shows that the sum terms, $\Delta E_{CT} + \Delta E_{POL}$, calculated with the ALMO-EDA, BLW, and NEDA methods, correlate linearly with the BOVB values with reasonably good correlation coefficients R^2 = 0.94−0.95. Figure S2 in the Supporting Information shows that the methods correlate with one another (ALMO vs NEDA, BLW vs NEDA, and ALMO vs BLW) with almost identical correlation coefficients.

Furthermore, the same sum terms calculated with ALMO[25] using three different density functional theory (DFT) functionals (ωB97X-D, B3LYP, and ωB97M-rV) agree very closely (see Table S14 in the Supporting Information). As such, it is reasonable to assume that the ΔE_{POL} and ΔE_{CT} terms in the sum terms are interlinked and represent the major stabilizing factor of the HB.

Strengths of the HB and Its Relation to the Charge-Shift Resonance Energy. As we described, the mixing of structures **3**−**5**/**3**$_a$−**5**$_a$ gives rise to the resonance energy of the HB moiety B----H in B----H−A. Thus, structure **4**/**4**$_a$ is the covalent Heitler−London structure of the B----H bond, whereas structures **3**/**3**$_a$ and **5**/**5**$_a$ are the corresponding ionic structures. As such, the VB mixing of these three structures at the optimized HB distance (B----H) gives rise to the total charge-shift resonance energy (RE_{CS})[3,33] of the HB.

Table 2 shows the BOVB calculated RE_{CS} for the nine HBs as well as ΔE_{diss} computed by BOVB and CCSD(T) methods. In each case, the RE_{CS} is determined relative to the VB structure of the lowest energy among **3**−**5**/**3**$_a$−**5**$_a$. Thus, for example, for $(F{---}H{---}F)^-$, the lowest structure is the triple-ion structure **3**$_a$. The RE_{CS} and ΔE_{diss} quantities in Table 2 are not identical, primarily because of the dissociation limit at which

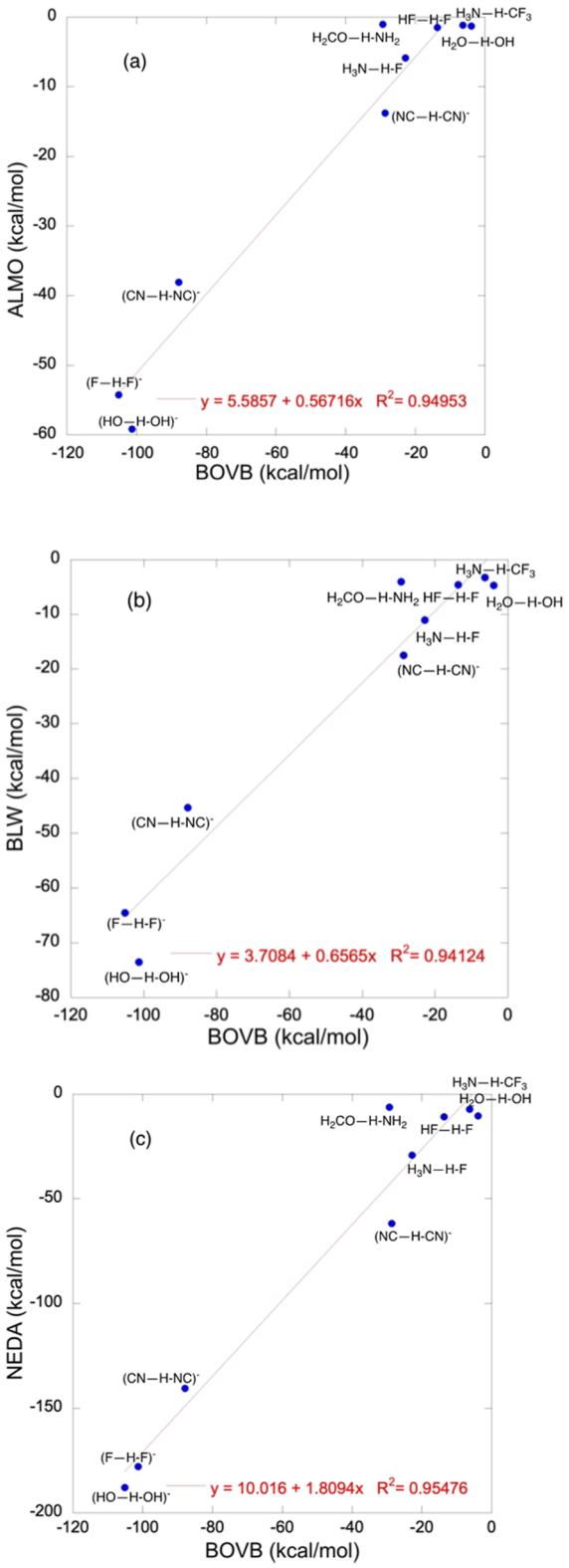

Figure 4. Plots of the sum terms, $\Delta E_{POL} + \Delta E_{CT}$, for HBs **1**−**9**: (a) ALMO versus BOVB. (b) BLW versus BOVB. (c) NEDA versus BOVB.

the ΔE_{diss} value is determined relative to the separated entities, for example, F^- + H−F in the case of $(F{---}H{---}F)^-$, whereas the reference for the RE_{CS} is the lowest VB structure (e.g., the triple-ion $F^-{---}H^+{---}F^-$). Other differences originate in the geometries of the fragments; RE_{CS} is determined by the use of

https://doi.org/10.1021/jacs.3c08196
J. Am. Chem. Soc. 2023, 145, 20132−20140

Table 2. RE_{CS} for the B----H Portion of the HBs and the Total ΔE_{diss} Values for VB(6)[a]

HB	1	2	3	4	5	6	7	8	9
RE_{CS}	3.7	7.2	6.2	6.8	14.3	20.9	41.5	62.8	65.6
ΔE_{diss} [b]	3.1	6.0	6.5	7.4	15.4	21.5	29.2	38.0	58.9
ΔE_{diss} [c]	3.1	5.8	4.9	5.3	13.0	22.8	31.9	38.6	54.4
ΔE_{diss} [d]	3.5	6.7	5.8	5.8	13.9	23.1	33.2	41.7	56.2

[a]All the energy values are in kcal/mol. [b]Corresponds to BOVB/6-311G(p,d). [c]Corresponds to CCSD(T)/cc-pVTZ. [d]Corresponds to CCSD(T)/6-311G(p,d).

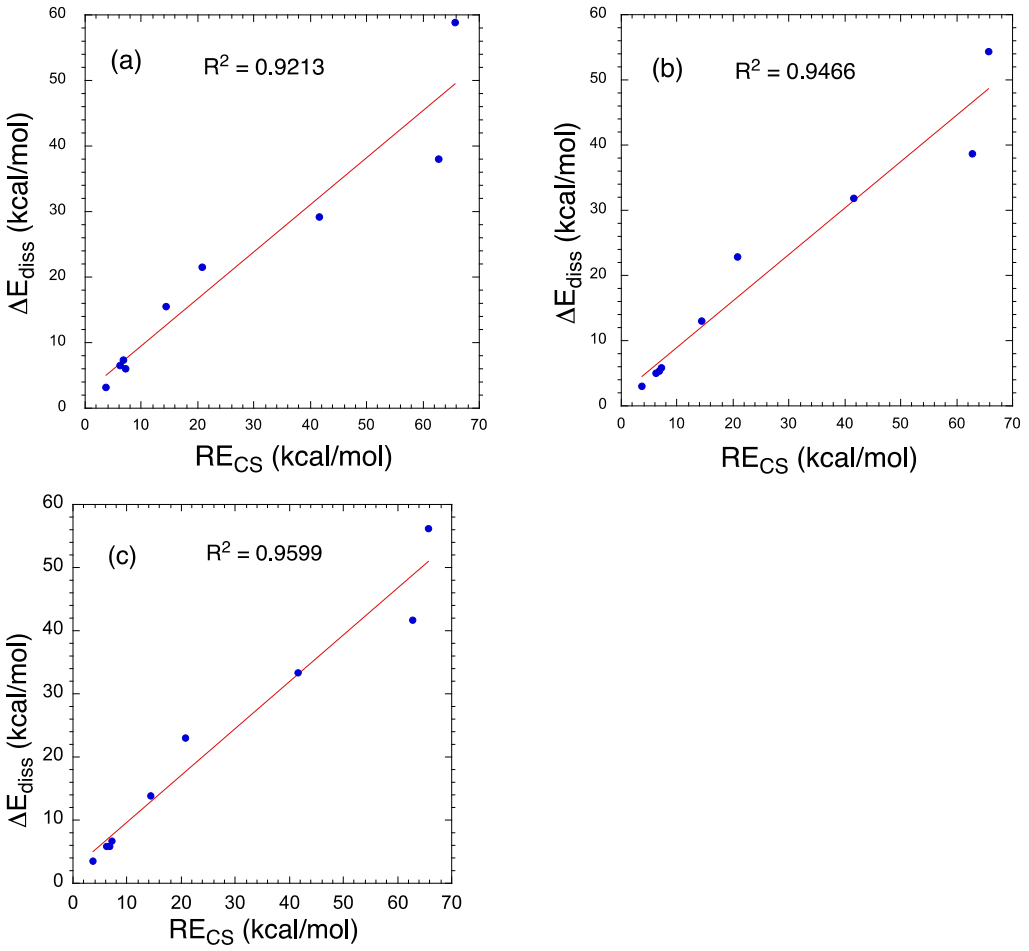

Figure 5. Correlations between RE_{CS} [BOVB/6-311G(p,d)] quantities for the B---H bond of the HB versus ΔE_{diss} values of the HBs using (a) BOVB/6-311G(p,d), (b) CCSD(T)/cc-pVTZ, and (c) CCSD(T)/6-311G(p,d). All values are in kcal/mol.

frozen fragment geometries as in the HB, whereas ΔE_{diss} uses relaxed fragment geometries.

Furthermore, as shown in Figure 5, the RE_{CS} quantities correlate with the dissociation energies (ΔE_{diss}) of the corresponding HBs (R^2 = 0.92−0.95). In principle, therefore, the VB-determined resonance energy of the HB (RE_{CS}) correlates with an experimentally relevant quantity, ΔE_{diss}, which gauges the thermodynamic stability of the HB. We regard this behavior as another advance in our understanding of the nature of the HB.

HBs as Drivers of Chemical Reactivity. As described above, some of the HBs in Figure 1 (e.g., the water dimer, **2**, $H_3N{-}H{-}CF_3$, **3**, and $H_3N{---}H{-}F$, **5**) carry larger positive charges on the external H atoms (which are not H-bonded) compared with the charges in the free molecules or those infinitely separated (i.e., 10 Å). This feature arises owing to the contribution of VB structure **4** (e.g., $H_2O^{\bullet+}$— $^{\bullet}H{:}OH^{-}$), which makes a significant contribution to the bond makeup of the HB of the water dimer and induces positive charging of the external H's (the same applies to the other neutral HBs mentioned above).

The charge differences between the external and free Hs are small, but they persist in all of the calculations we used. To further test this phenomenon, we optimized the water tetramer $(H_2O)_4$ and the free H_2O molecule using the MP2/cc-pVTZ level of theory and found the trend to persist. The resulting NBO/CCSD charges of the external Hs are 0.454 (0.470) versus 0.444 (0.462) in the free molecule; the parenthetical values refer to charges in an aqueous solution. In a water droplet, these external $O{-}H^{\delta+}$ bonds generate electric fields (EFs), which are normal to the surface of the droplet and can lead to unexpected redox reactions.

Recently, Head-Gordon et al.,[26f] used coarse-grained electron modeling of a water droplet and reported that the

https://doi.org/10.1021/jacs.3c08196
J. Am. Chem. Soc. 2023, 145, 20132−20140

fluctuations of the EFs at the surface of the droplet are much larger than the interior of the droplet. When the environmental EF distributions are projected onto the O−H bonds found in the interior versus the surface of a water droplet, the droplet surface EFs of ∼16 MV/cm yield enough power to lower the activation energy to accelerate the rates of chemical reactions by several orders of magnitude.

Zare et al.[5,26e,g] showed that water droplets promote a variety of unusual reactions. Thus, water droplets on silica surfaces or in aqueous reactions lead to contact electrification and the generation of H_2O_2, which oxidizes organic molecules.[5] Even when spraying from bulk water, the water droplets lead to the reduction of a variety of organic molecules.[26e] Other groups[26a−d,f] have expressed similar observations/conclusions.

Clearly, the importance of HBs extends from structural/mechanical effects to the enabling of unusual reactions.

CONCLUSIONS

VBT is used to unify the bonding aspects of the HB in a series of HBs that range from weak to strong ones that are nearly symmetric[24] [e.g., $(HO{-}{-}{-}H{-}{-}{-}OH)^-$ and $(FHF)^-$].

The two major interactions that make up HBs are due to POL and CT, which are caused by the significant involvement of the ionic VB structures (Scheme 3) in bonding. The sum POL + CT displays the same pattern (displayed in Figure 3), irrespective of which term is actually larger or smaller. Furthermore, the sum terms for VBT correlate linearly (Figure 4) with the corresponding ones obtained from various EDA methods tested in this paper: ALMO (using Hartree-Fock and three different functionals),[25] BLW,[16,17] and NEDA.[20]

Additionally, the VB analysis reveals that the RE_{CS} of the B----H portion of the B:----HA HB correlates linearly with the dissociation energy of the HB, ΔE_{diss} (Figure 5). As such, RE_{CS} values can, in principle, be extracted from plots against experimental ΔE_{diss} values.

Finally, in agreement with MP2 and CCSD, VBT reveals that the contributions of ionic structures to the HB increase the positive charge on the hydrogen of the corresponding external O−H bonds in the water dimer, compared with a free water molecule. This increases the EF of the external O−H bonds of water droplets and of water in contact with hydrophobic media, such as air, oil, or a metal oxide surface. In all these cases, the EF of the external O−H bond has been shown to enable chemical reactions not found in bulk water.[5,26]

Thus, HBs are multifaceted. The HB constitutes a key architectural element of ice, proteins, nucleic acids, and many other structures; it is responsible for the stability of aggregates of small molecules;[8,9] and it endows materials with special mechanical properties in solution, solids, and in soft matter such as proteins and polymers.[10] Moreover, HBs possess bonding aspects that are more intriguing than isolated bonds in molecules. These bonding mechanisms hold together the HB components by means of significant charge-shift resonance energies, and they electrify Hs in interfaces of water−air/solid/oily matter and endow the HBs with increased reactivity.

ASSOCIATED CONTENT

Supporting Information

The Supporting Information is available free of charge at https://pubs.acs.org/doi/10.1021/jacs.3c08196.

VB diagrams; VB structures; BOVB, MP2, and CCSD(T) computational data; and CCSD(T) calculated *XYZ* coordinates (PDF)

AUTHOR INFORMATION

Corresponding Authors

Sason Shaik − *Institute of Chemistry, The Hebrew University of Jerusalem, Jerusalem 9190401, Israel;* orcid.org/0000-0001-7643-9421; Email: sason.shaik@gmail.com

Richard N. Zare − *Department of Chemistry, Stanford University, Stanford, California 94305, United States;* orcid.org/0000-0001-5266-4253; Email: rnz@stanford.edu

Author

David Danovich − *Institute of Chemistry, The Hebrew University of Jerusalem, Jerusalem 9190401, Israel;* orcid.org/0000-0002-8730-5119

Complete contact information is available at: https://pubs.acs.org/10.1021/jacs.3c08196

Author Contributions

The manuscript was written through the contributions of all authors.

Funding

S.S. thanks the Israeli Science Foundation (ISF grant 520/18) for financial support. R.N.Z. thanks the US Air Force Office of Scientific Research through the Multidisciplinary University Research Initiative program (AFOSR FA9550-21-1-0170).

Notes

The authors declare no competing financial interest.

ACKNOWLEDGMENTS

Jilai Li is thanked for his advice on the elephant parable.

DEDICATION

This paper is dedicated to Roald Hoffmann on the occasion of his 85th birthday.

ABBREVIATIONS

BOVB	breathing-orbital valence bond method
VBT	valence bond theory
EDA	energy decomposition analysis
HB	hydrogen bonding
RE	resonance energy
BLW	block-localized wavefunction
NBO	natural bond orbital
ALMO	absolutely localized molecular orbitals
NEDA	natural energy decomposition analyses
EF	electric field

REFERENCES

(1) Arunan, E.; Desiraju, G. R.; Klein, R. A.; Sadlej, J.; Scheiner, S.; Alkorta, I.; Clary, D. C.; Crabtree, R. H.; Dannenberg, J. J.; Hobza, P.; Kjaergaard, H. G.; Legon, A. C.; Mennucci, B.; Nesbitt, D. J. Definition of the Hydrogen Bond (IUPAC Recommendations 2011). *Pure Appl. Chem.* **2011**, *83*, 1637−1641.

(2) Shaik, S. Helmut Schwarz—A Story of Science and Friendship. *Int. J. Mass Spectrom.* **2019**, *435*, 151−162.

(3) Shaik, S.; Danovich, D.; Galbraith, J. M.; Braida, B.; Wu, W.; Hiberty, P. C. Charge-Shift Bonding: A New and Unique Form of Bonding. *Angew. Chem., Int. Ed.* **2020**, *132*, 996−1013.

(4) Shaik, S.; Hiberty, P. C. *A Chemist's Guide to Valence Bond Theory*; Wiley-Interscience, Wiley & Sons, Inc.: Hobboken, New Jersey, USA, 2008.
(5) Chen, B.; Xia, Y.; He, R.; Sang, H.; Zhang, W.; Li, J.; Chen, L.; Wang, P.; Guo, S.; Yin, Y.; Hu, L.; Song, M.; Liang, Y.; Wang, Y.; Jiang, G.; Zare, R. N. Water-Solid Contact Electrification Causes Hydrogen Peroxide Production from Hydroxyl Radical Recombination in Sprayed Microdroplets. *Proc. Natl. Acad. Sci. U.S.A.* **2022**, *119*, No. e220905619.
(6) (a) Latimer, W. M.; Rodebush, W. H. Polarity and Ionization from the Standpoint of the Lewis Theory of Valence. *J. Am. Chem. Soc.* **1920**, *42*, 1419−1433. (b) Lewis, G. N. *Valence and the Structure of Atoms and Molecules*; The Chemical Catalog Co., Inc.: New York, USA, 1923; pp 109−111.
(7) (a) Pauling, L. The Shared-Electron Chemical Bond. *Proc. Natl. Acad. Sci. U.S.A.* **1928**, *14*, 359−362. (b) Pauling, L. *The Nature of the Chemical Bond*, 3rd ed.; Cornell University Pres: Ithaca, New York, 1960; p 452.
(8) Jeffrey, D. A. *An Introduction to Hydrogen Bonding*; Oxford University Press: New York, 1997.
(9) (a) For historical details see: Goymer, P. 100 Years of the Hydrogen Bond. *Nat. Chem.* **2012**, *4*, 863−864. (b) See also H. Rzepa's blog: DOI: 10.14469/hpc/10731 and https://doi.org/10.14469/hpc/10732; DOI: 10.14469/hpc/10512 and https://doi.org/10.14469/hpc/10382. (c) HBs in polypeptides: Pauling, L.; Corey, R. B. Configurations of Polypeptide Chains With Favored Orientations Around Single Bonds. *Proc. Natl. Acad. Sci. U.S.A.* **1951**, *37*, 729−740. (d) Pauling, L.; Corey, R. B.; Branson, H. R. The Structure of Proteins: Two Hydrogen-Bonded Helical Configurations of the Polypeptide Chain. *Proc. Natl. Acad. Sci. U.S.A.* **1951**, *37*, 205−211. (e) For a general review: Pauling, L. *The Nature of the Chemical Bond*, 3rd ed.; Cornell University Press: Ithaca, New York, 1960; pp 450−504. (f) Reed, A. E.; Curtiss, L. A.; Weinhold, F. Intermolecular Interactions from a Natural Bond Orbital, Donor-Acceptor Viewpoint. *Chem. Rev.* **1988**, *88*, 899−926. (g) For the Importance of HBs in Catalysis of Organic Reactions, see: Schreiner, P. R. Metal-Free Organocatalysis through Explicit Hydrogen Bonding Interactions. *Chem. Soc. Rev.* **2003**, *34*, 289−296. (h) For a general review: Grabowski, S. J. What Is the Covalency of Hydrogen Bonding? *Chem. Rev.* **2011**, *111*, 2597−2625. (i) Steiner, T. The Hydrogen Bond in the Solid State. *Angew. Chem., Int. Ed.* **2002**, *41*, 48−76. (j) Hubbard, R. E.; Kamran Haider, M. Hydrogen Bonds in Proteins: Role and Strength. *Encyclopedia of Life Sciences (ELS)*. John Wiley & Sons, Ltd: Chichester, 2010.
(10) (a) Li, W.; Ma, J.; Wu, S.; Zhang, J.; Cheng, J. The Effect of Hydrogen Bond on the Thermal and Mechanical Properties of Furan Epoxy Resins: Molecular Dynamics Simulation Study. *Polym. Test.* **2021**, *101*, 107275−107288. (b) Monk, J. D.; Bucholz, E. W.; Boghozian, T.; Deshpande, S.; Schieber, J.; Bauschlicher, C. W., Jr.; Lawson, J. W. Computational and Experimental Study of Phenolic Resins: Thermal−Mechanical Properties and the Role of Hydrogen Bonding. *Macromolecules* **2015**, *48*, 7670−7680. (c) Vener, M.; Egorova, A.; Tsirelson, V.; Egorova, A. N.; Tsirelson, V. G. Hydrogen Bonds and O—O Interactions in Proton-Ordered Ices. DFT Computations with Periodic Boundary Conditions. *Chem. Phys. Lett.* **2010**, *500*, 272−276. (d) For molecular dynamics of binding affinities in ligand-protein complexes: Yunta, M. J. R. It is Important to Compute Intramolecular Hydrogen Bonding in Drug Design? *Am. J. Model. Optim.* **2017**, *5*, 24−57. (e) Schneider, H.-J. Hydrogen Bonds with Fluorine. Studies in Solution, in Gas Phase and by Computations, Conflicting Conclusions from Crystallographic Analyses. *Chem. Sci.* **2012**, *3*, 1381−1394. (f) For piezoelectric effects due to HBs in piezoelectric materials: Werling, K. A.; Griffin, M.; Hutchison, G. R.; Lambrecht, D. S. Piezoelectric Hydrogen Bonding: Computational Screening for a Design Rationale. *J. Phys. Chem. A* **2014**, *118*, 7404−7410.
(11) Grabowski, S. J. Hydrogen and Halogen Bonds are Ruled by the Same Mechanisms. *Phys. Chem. Chem. Phys.* **2013**, *15*, 7249−7259.
(12) (a) Pendas, A. M.; Blanc, M. A.; Francisco, E. The Nature of the Hydrogen Bond: A Synthesis from the Interacting Quantum Atoms Picture. *J. Chem. Phys.* **2006**, *125*, 184112−184119. (b) For discussions of path dependency of EDA, see: Andrada, D. M.; Foroutan-Nejad, C. Energy Components in Energy Decomposition Analysis (EDA) are Path Functions; Why does it Matter? *Phys. Chem. Chem. Phys.* **2020**, *22*, 22459−22464. (c) Poater, J.; Andrada, D. M.; Sola, M.; Foroutan-Nejad, C. Path-Dependency of Energy Decomposition Analysis & the Elusive Nature of Bonding. *Chem. Chem. Phys.* **2022**, *24*, 2344−2348. (d) On limitations of EDA analyses, see: Vojtech, S.; Sowlati-Hashjin, S.; Karttunen, M.; Pendas, A. M.; Foroutan-Nejad, C. Reply to: On the existence of collective interactions reinforcing the metal-ligand bond in organometallic compounds. *Nat. Commun.* **2023**, *14*, 3873.
(13) (a) Morokuma, K. The Origin of Hydrogen Bonding. An Energy Decomposition Study. *Acc. Chem. Res.* **1977**, *10*, 294−300. (b) Umeyama, H.; Morokuma, K. The Origin of Hydrogen Bonding. An Energy Decomposition Study. *J. Am. Chem. Soc.* **1977**, *99*, 1316−1332. (c) Kitaura, K.; Morokuma, K. A New Energy Decomposition Scheme for Molecular Interactions within the Hartree-Fock Approximation. *Int. J. Quantum Chem.* **1976**, *10*, 325−340.
(14) Ziegler, T.; Rauk, A. A. Theoretical Study of the Ethylene-Metal Bond in Complexes between Cu^+, Ag^+, Au^+, Pt°, or Pt^{2+} and Ethylene, Based on the Hartree-Fock-Slater Transition-State Method. *Inorg. Chem.* **1979**, *18*, 1558−1565.
(15) Bickelhaupt, F. M.; Baerends, E. J. Kohn-Sham Density Functional Theory: Predicting and Understanding Chemistry. *Rev. Comput. Chem.* **2000**, *15*, 1−86.
(16) (a) Mo, Y.; Gao, J.; Peyerimhoff, S. D. Energy Decomposition Analysis of Intermolecular Interactions using a Block-Localized Wavefunction Approach. *Chem. Phys.* **2000**, *112*, 5530−5538. (b) Mo, Y.; Song, L.; Lin, Y. Block-Localized Wavefunction (BLW) Method at the Density Functional Theory (DFT) Level. *J. Phys. Chem. A* **2007**, *111*, 8291−8301.
(17) (a) Beck, J. F.; Mo, Y. How Resonance Assists Hydrogen Bonding Interactions: An Energy Decomposition Analysis. *J. Comput. Chem.* **2007**, *28*, 455−466. (b) Mo, Y.; Wang, C.; Guan, L.; Braïda, B.; Hiberty, P. C.; Wu, W. On the Nature of Blue Shifting Hydrogen Bonds. *Chem.—Eur. J.* **2014**, *20*, 8444−8452. (c) Chang, X.; Zhang, Y.; Weng, X.; Su, P.; Wu, W.; Mo, Y. Red-Shifting versus Blue-Shifting Hydrogen Bonds: Perspective from Ab Initio Valence Bond Theory. *J. Phys. Chem. A* **2016**, *120*, 2749−2756.
(18) Foster, J. P.; Weinhold, F. Natural Hybrid Orbitals. *J. Am. Chem. Soc.* **1980**, *102*, 7211−7218.
(19) (a) Weinhold, F.; Klein, R. A. What is a Hydrogen Bond? Mutually Consistent Theoretical and Experimental Criteria for Characterizing H-bonding Interactions. *Mol. Phys.* **2012**, *110*, 565−579. (b) Weinhold, F. Nature of H-bonding in Clusters, Liquids, and Enzymes: An ab Initio, Natural Bond Orbital Perspective. *J. Mol. Struct.* **1997**, *398*−*399*, 181−197. (c) Weinhold, F.; Klein, R. A. What is a Hydrogen Bond? Resonance Covalency in the Supramolecular Domain. *Chem. Educ. Res. Pract.* **2014**, *15*, 276−285. (d) Weinhold, F.; Klein, R. A. Anti-Electrostatic Hydrogen Bonds. *Angew. Chem., Int. Ed.* **2014**, *53*, 11214−11217.
(20) (a) Glendening, E. D.; Streitwieser, A., Jr. Natural Energy Decomposition Analysis: An Energy Partitioning Procedure for Molecular Interactions with Application to Weak Hydrogen Bonding, Strong Ionic, and Moderate Donor−Acceptor Interactions. *J. Chem. Phys.* **1994**, *100*, 2900−2909. (b) Schenter, G. K.; Glendening, E. D. Natural Energy Decomposition Analysis: The Linear Response Electrical Self Energy. *J. Phys. Chem.* **1996**, *100*, 17152−17156. (c) Glendening, E. D. Natural Energy Decomposition Analysis: Explicit Evaluation of Electrostatic and Polarization Effects with Application to Aqueous Clusters of Alkali Metal Cations and Neutrals. *J. Am. Chem. Soc.* **1996**, *118*, 2473−2482. (d) For NEDA/DFT, see: Glendening, E. D. Natural Energy Decomposition Analysis: Extension to Density Functional Methods and Analysis of Cooperative Effects in Water Clusters. *J. Phys. Chem. A* **2005**, *109*, 11936−11940. (e) Glendening, E. D.; Badenhoop, J. K.; Reed, A. E.; Carpenter, J.

https://doi.org/10.1021/jacs.3c08196
J. Am. Chem. Soc. 2023, 145, 20132−20140

E.; Bohmann, J. A.; Morales, C. M.; Weinhold, F. *NBO 5.0*; Theoretical Chemistry Institute, University of Wisconsin: Madison, 2001.
(21) (a) Wang, C.; Danovich, D.; Mo, Y.; Shaik, S. On The Nature of the Halogen Bond. *J. Chem. Theory Comput.* **2014**, *10*, 3726−3737. (b) Wang, C.; Danovich, D.; Shaik, S.; Mo, Y. Halogen Bonds in Novel Polyhalogen Monoanions. *Chem.—Eur. J.* **2017**, *23*, 8719−8728.
(22) (a) Clark, T. σ-Holes. *Wiley Interdiscip. Rev.: Comput. Mol. Sci.* **2013**, *3*, 13−20. (b) Murray, J. S.; Politzer, P. Molecular Electrostatic Potentials and Noncovalent Interactions. *Wiley Interdiscip. Rev.: Comput. Mol. Sci.* **2017**, *7*, No. e1326. (c) Murray, J. S.; Politzer, P. Hydrogen Bonding A Coulombic σ-Hole Interaction. *J. Indian Inst. Sci.* **2020**, *100*, 1121−1130.
(23) (a) Bader, R. F. W. A. A quantum theory of molecular structure and its applications. *Chem. Rev.* **1991**, *91*, 893−928. (b) Bader, R. F. W. *Atoms in Molecules, A Quantum Theory*; Oxford University Press: Oxford, 1990. (c) *Quantum Theory of Atoms in Molecules: From Solid State to DNA and Drug Design*; Matta, C. F., Boyd, R. J., Eds.; Wiley VCH: Weinheim, 2007. (d) Matta, C. F.; Bader, R. F. W. An Experimentalist's Reply to "What Is an Atom in a Molecule?". *J. Phys. Chem. A* **2006**, *110*, 6365−6371. (e) Matta, C. F. How Dependent are Molecular and Atomic Properties on the Electronic Structure Method? Comparison of Hartree-Fock, DFT, and MP2 on a Biologically Relevant Set of Molecules. *J. Comput. Chem.* **2010**, *31*, 1297−1311.
(24) For the symmetric solid state structure of the anion [HO---H---OH]−, see: Bino, A.; Gibson, D. A New Bridging Ligand, the Hydrogen Oxide Ion ($H_3O_2^-$). *J. Am. Chem. Soc.* **1981**, *103*, 6741−6742.
(25) (a) Levine, D. S.; Horn, P. R.; Mao, Y.; Head-Gordon, M. Variational Energy Decomposition Analysis of Chemical Bonding. 1. Spin-Pure Analysis of Single Bonds. *J. Chem. Theory Comput.* **2016**, *12*, 4812−4820. (b) Levine, D. S.; Head-Gordon, M. Energy decomposition analysis of single bonds within Kohn−Sham density functional theory. *Proc. Natl. Acad. Sci. U.S.A.* **2017**, *114*, 12649−12656.
(26) (a) Nandy, A.; Kumar, A.; Mondal, S.; Koner, D.; Banerjee, S. Spontaneous Generation of Aryl Carbocations from Phenols in Aqueous Microdroplets: Aromatic S_N1 Reactions at the Air-Water Interface. *J. Am. Chem. Soc.* **2023**, *145*, 15674−15679. (b) Ben-Amotz, D. Electric Buzz in a Glass of Pure Water. *Science* **2022**, *376*, 800−801. (c) Schran, C.; Marsalek, O.; Markland, T. E. Unravelling the Influence of Quantum Proton Delocalization on Electronic Charge Transfer Through the Hydrogen Bond. *Chem. Phys. Lett.* **2017**, *678*, 289−295. (d) Poli, E.; Jong, K. H.; Hassanali, A. Charge transfer as a Ubiquitous Mechanism in Determining the Negative Charge at Hydrophobic Interfaces. *Nat. Commun.* **2020**, *11*, 901−913. (e) Lee, J. K.; Samanta, D.; Nam, H. G.; Zare, R. N. Micrometer-Sized Water Droplets Induce Spontaneous Reduction. *J. Am. Chem. Soc.* **2019**, *141*, 10585−10589. (f) Hao, H.; Leven, I.; Head-Gordon, T. Can Electric Field Drive Chemistry for an Aqueous Microdroplet? *Nat. Commun.* **2022**, *13*, 280−288. (g) Mehrgardi, M. A.; Mofidfar, M.; Zare, R. N. Sprayed Water Microdroplets Are Able to Generate Hydrogen Peroxide Spontaneously. *J. Am. Chem. Soc.* **2022**, *144*, 7606−7609.
(27) (a) For Møller−Plesset Second Order Perturbation Theory (MP2), see: Frisch, M. J.; Head-Gordon, M.; Pople, A. A Direct MP2 Gradient Method. *Chem. Phys. Lett.* **1990**, *166*, 275−280. (b) Head-Gordon, M.; Head-Gordon, T. Analytic MP2 Frequencies Without Fifth Order Storage: Theory and Application to Bifurcated Hydrogen Bonds in the Water Hexamer. *Chem. Phys. Lett.* **1994**, *220*, 122−128.
(28) For Coupled-Cluster theory with single- and double-configurations corrections, and perturbation theoretic treatment of triples, see: Raghavachari, K.; Trucks, G. W.; Pople, J. A.; Head-Gordon, M. A Fifth-order Perturbation Comparison of Electron Correlation Theories. *Chem. Phys. Lett.* **1989**, *157*, 479−483.
(29) (a) cc-pVTZ: Dunning, T. H., Jr. Gaussian Basis Sets for Use in Correlated Molecular Calculations. I. The Atoms Boron Through Neon and Hydrogen. *J. Chem. Phys.* **1989**, *90*, 1007−1023. (b) 311G(p,d): Raghavachari, K.; Binkley, J. S.; Seeger, R.; Pople, J. A. Self-Consistent Molecular Orbital Methods. 20. Basis Set for Correlated Wave-Functions. *J. Chem. Phys.* **1980**, *72*, 650−654.
(30) (a) Song, L.; Mo, Y.; Zhang, Q.; Wu, W. XMVB: A Program for Ab Initio Nonorthogonal Valence Bond Computations. *J. Comput. Chem.* **2005**, *26*, 514−521. (b) Chen, Z.; Ying, F.; Chen, X.; Song, J.; Su, P.; Song, L.; Mo, Y.; Zhang, Q.; Wu, W. XMVB 2.0: A New Version of Xiamen Valence Bond Program. *Int. J. Quantum Chem.* **2015**, *115*, 731−737.
(31) For the leading BOVB references, see: (a) Hiberty, P. C.; Flament, J. P.; Noizet, E. Compact and Accurate Valence Bond Functions with Different Orbitals for Different Configurations: Application to the Two-Configuration Description of F_2. *Chem. Phys. Lett.* **1992**, *189*, 259−265. (b) Hiberty, P. C.; Shaik, S. Breathing-Orbital Valence Bond Method - a Modern Valence Bond Method that Includes Dynamic Correlation. *Theor. Chem. Acc.* **2002**, *108*, 255−272. (c) Van Lenthe, J. H.; Balint-Kurti, G. G. The Valence-Bond Self-Consistent Field Method (VB-SCF): Theory and Test Calculations. *J. Chem. Phys.* **1983**, *78*, 5699−5713.
(32) Shaik, S.; Shurki, A. Valence Bond Diagrams and Chemical Reactivity. *Angew. Chem., Int. Ed.* **1999**, *38*, 586−625.
(33) Shaik, S.; Danovich, D.; Hiberty, P. C. The Nature of the Chemical Bond According to Valence Bond Theory. *J. Chem. Phys.* **2022**, *157*, 090901.

https://doi.org/10.1021/jacs.3c08196
J. Am. Chem. Soc. 2023, 145, 20132−20140